

## **Recurrent Antecedent Hypoglycemia Alters Neuronal Oxidative Metabolism in Vivo**

Running title: Brain metabolic adaptations to recurrent hypoglycemia

Lihong Jiang<sup>1\*</sup>, Raimund I. Herzog<sup>2\*</sup>, Graeme F. Mason<sup>1,3</sup>, Robin A. de Graaf<sup>1</sup>, Douglas L. Rothman<sup>1</sup>, Robert S. Sherwin<sup>2</sup> and Kevin L. Behar<sup>3</sup>

Departments of Diagnostic Radiology<sup>1</sup>, Internal Medicine<sup>2</sup>, and Psychiatry<sup>3</sup>, Magnetic Resonance Research Center, Yale University School of Medicine, The Anlyan Center, New Haven, Connecticut 06520

\*L.J. and R.I.H. contributed equally to this article

**Corresponding author:**  
Dr. Lihong Jiang,  
Email: [lihong.jiang@yale.edu](mailto:lihong.jiang@yale.edu)

Additional information for this article can be found in an online appendix at  
<http://diabetes.diabetesjournals.org>

Submitted 2 December 2008 and accepted 2 March 2009.

This is an uncopyedited electronic version of an article accepted for publication in *Diabetes Care*. The American Diabetes Association, publisher of *Diabetes Care*, is not responsible for any errors or omissions in this version of the manuscript or any version derived from it by third parties. The definitive publisher-authenticated version will be available in a future issue of *Diabetes Care* in print and online at <http://diabetes.diabetesjournals.org>.

**Objective-** To characterize the changes in brain metabolism caused by antecedent recurrent hypoglycemia under euglycemic and hypoglycemic conditions in a rat model, and test the hypothesis that recurrent hypoglycemia changes the brain's capacity to utilize different energy substrates.

**Research design and methods-** Rats exposed to recurrent insulin-induced hypoglycemia for 3 days (3dRH) and untreated controls were subject to the following protocols: [2-<sup>13</sup>C]-acetate infusion under euglycemic conditions (n=8), [1-<sup>13</sup>C]-glucose and unlabeled acetate co-infusion under euglycemic conditions (n=8), and [2-<sup>13</sup>C]-acetate infusion during a hyperinsulinemic-hypoglycemic clamp (n=8). *In vivo* nuclear magnetic resonance spectroscopy was employed to monitor the rise of <sup>13</sup>C-labeling in brain metabolites for the calculation of brain metabolic fluxes using a neuron-astrocyte model.

**Results-** At euglycemia, antecedent recurrent hypoglycemia increased whole brain glucose metabolism by 43±4% (p<0.01 vs controls), largely due to higher glucose utilization in neurons. While acetate metabolism remained the same, control and 3dRH animals showed a distinctly different response to acute hypoglycemia: Controls decreased pyruvate dehydrogenase-(PDH)-flux in astrocytes by 64±20% (p=0.01), whereas it increased by 37±3% in neurons (p=0.01). The 3dRH animals decreased PDH-flux in both compartments (-75±20% in astrocytes, p<0.001 and -36±4% in neurons, p=0.005). Thus, acute hypoglycemia reduced total brain TCA cycle activity in 3dRH animals (-37±4% p=0.001), but not in controls.

**Conclusion-** Our findings suggest that after antecedent hypoglycemia glucose utilization is increased at euglycemia and decreased after acute hypoglycemia, which was not the case in controls. These findings may help to identify better methods of preserving brain function and reducing injury during acute hypoglycemia.

Large clinical trials have established that the long term complications of diabetes can be mitigated by tight glycemic control (1; 2). Intensive insulin therapy, however, is limited by an increased risk of severe hypoglycemia which results, in large part from a blunting of counterregulatory responses as well as reduced awareness of hypoglycemia (3-6). Characterization of the underlying metabolic adaptations involved could lead to new therapeutic approaches aimed at improving glycemic control without compromising the risk of severe hypoglycemia.

Impaired judgment and decreased memory function during acute hypoglycemia are thought to be consequences of alterations of brain energy metabolism, in particular the absence of glucose, the primary energy substrate for the brain (7; 8). The blunting of epinephrine and glucagon responses to hypoglycemia observed in type 1 diabetic patients exposed to frequent hypoglycemic episodes are reproduced in animal models of recurrent antecedent insulin-induced hypoglycemia, suggesting that such models may offer insights into the metabolic adaptations observed in the clinical setting (9-11). Studies of cognitive performance using a spatial memory task in non-diabetic and diabetic rats exposed to recurrent hypoglycemia on three consecutive days (3dRH) and in non-diabetic animals exposed to weekly bouts of hypoglycemia for nearly a year have revealed better performance at euglycemia, suggesting that adaptations of brain glucose transport and/or metabolism are similar to those reported for diabetic patients (9; 10). These studies suggest that our animal models may offer insights into the metabolic

adaptations observed in the clinical setting (9; 11; 12).

It is also possible that when the brain is repeatedly deprived of its main energy substrate, glucose, its capacity to take up and utilize alternate fuels such as monocarboxylic acids or ketone bodies is increased. This view is supported by a recent NMR spectroscopy study that demonstrated an increase in acetate metabolism in type 1 diabetic patients with hypoglycemia unawareness (13). In contrast, rodents exposed to recurrent hypoglycemia for 3 consecutive days (3dRH) under hypoglycemic conditions performed worse on a memory task than saline injected controls(9).

The present study was undertaken to assess the effects of antecedent recurrent hypoglycemia on the brain's capacity to oxidize glucose and an alternate fuel (acetate). Three different experiments were conducted using both, control and 3dRH animals: (1) First we measured neuronal and astroglial metabolic fluxes under euglycemic conditions using [2-<sup>13</sup>C]-acetate, which is primarily metabolized by astroglia labeling neurons through the glutamate/glutamine neurotransmitter cycle. The accumulation of label in the stable metabolite pools of glutamine (Gln) and glutamate (Glu) was monitored by localized <sup>1</sup>H-observed, <sup>13</sup>C-edited (<sup>1</sup>H-[<sup>13</sup>C]) NMR spectroscopy. This approach, when used in conjunction with a two compartment mathematical model of brain metabolism (Figure 1), allows the quantitation of the rates of neuronal and glial TCA cycles, glutamate/glutamine neurotransmitter cycle, and other metabolic pathways in brain (13; 14). (2) Next, to more directly assess neuronal metabolism using a substrate which is predominately metabolized in neurons, we measured metabolic fluxes during

infusion of [1-<sup>13</sup>C]-glucose in conjunction with unlabeled acetate. (3) Lastly, metabolic fluxes were assessed during acute hypoglycemic-hyperinsulinemic clamp and [2-<sup>13</sup>C]acetate infusion to reveal the extent to which glucose and acetate contributes to brain oxidative metabolism when blood glucose is deficient.

## RESEARCH DESIGN AND METHODS

**Animals:** Male Sprague-Dawley rats (Charles River, Wilmington, MA) of 220g-250g were housed in the Yale Animal Resource Center, fed a standard pellet diet (AgwayProlab 3000, Syracuse, NY), and maintained on a 12-h day/night cycle. Experimental protocols were in accordance with laboratory animal care guidelines and were approved by the Yale Animal Care and Use Committee.

**Recurrent hypoglycemia:** Recurrent hypoglycemia was induced as previously described (15). Briefly, animals received i.p. injections of regular insulin (10U/kg Humulin R, Lilly, Indianapolis, IN) to produce 3hrs of hypoglycemia on 3 consecutive days, resulting in tail vein glucose levels of 30-40mg/dl. After three hours animals were given access to food and allowed to return to euglycemia. The following day NMR experiments were performed.

**Surgical Preparation:** During surgical preparation for *in vivo* NMR experiments animals were anesthetized with 3% halothane, underwent tracheotomy and were ventilated with a mixture of 30% O<sub>2</sub>/69% N<sub>2</sub>O/1% halothane via a small animal ventilation system (Harvard Apparatus, Holliston, MA). The left femoral artery was catheterized for continuous monitoring of blood pressure, plasma sampling, and blood gas analysis (see Table 1). Core body temperature was measured and maintained at 37±1°C

using a water heating pad. Both femoral veins were cannulated for infusion of insulin, glucose and acetate. Isotopically labeled substrates were infused into a separate line using computer-controlled pumps (Harvard Apparatus, Holliston, MA). Animals were then placed into a plastic holder with a surface coil positioned directly on top of the scalp for NMR experiments.

**Experimental Groups:** a) Euglycemia - acetate infusion. 2M [2-<sup>13</sup>C]-acetate (99% <sup>13</sup>C-sodium salt, Cambridge Isotopes, Andover, MA), at pH=7 was infused into 3dRH (n=8) and control (n=8) animals under basal euglycemic conditions. Animals had free access to food the night prior to the experiment to avoid significant ketone body accumulation. A bolus-continuous infusion of labeled acetate designed to produce steady state plasma levels was given according to the following protocol: 6.25µmol/min/g from 0 to 15s, 0.875µmol/min/g from 15s to 4min, 0.5µmol/min/g from 4 to 8min, and 0.25µmol/min/g thereafter. b) Euglycemia - glucose/acetate co-infusion. Because of the uncertainty associated with this method of determining V<sub>pdhN</sub> we performed a co-infusion study with [1-<sup>13</sup>C]-glucose and unlabeled acetate to measure V<sub>pdhN</sub> more directly. 1.1M [1-<sup>13</sup>C]-glucose (99% <sup>13</sup>C, Cambridge Isotopes, Andover, MA) was co-infused with 2M acetate into 3dRH (n=8) and control (n=8) animals under basal euglycemic conditions. Unlabeled acetate was infused in identical doses as in the protocol described above and 20minutes later [1-<sup>13</sup>C]-glucose was administered as a bolus of 4.05µmol/g/min for 15s followed by stepped exponential reduction of infusion rates every 30s for the next 8mins, arriving at a steady rate of 0.051µmol/g/min for the remainder of the experiment. Regular insulin

(50mU/kg/min) was used to during the initial 30 minutes to prevent plasma glucose from increasing in association with the labeled glucose infusion. c) Hypoglycemia - acetate infusion. 2M [2-<sup>13</sup>C]-acetate was infused into 3dRH (n=8) and control (n=8) animals during acute insulin-induced hypoglycemia. Animals were fasted overnight prior to a hyperinsulinemic-hypoglycemic clamp study (50mU/kg/min) in which a variable infusion of 20% dextrose (Hospira Inc., Lakeforest, IL) to was used to maintain plasma glucose at the target level of  $2.1 \pm 0.2$  mM (Figure 2a). Plasma glucose concentrations (Figure 2b) were measured every ten minutes in between NMR scans using a Beckman Glucose analyzer 2 (Beckman Coulter, Inc. Fullerton, CA). Infusion rates of labeled acetate were reduced by 20% as compared to the euglycemic studies in order to optimize physiological parameters such as blood pressure, blood pH, pO<sub>2</sub> and pCO<sub>2</sub>, this dose, however was sufficient for plasma acetate levels to saturate transport.

**NMR Spectroscopy:** Following placement of the animals into the scanner, *in vivo* NMR spectroscopy was performed during the respective infusions in a 9.4T horizontal bore magnet (Magnex, Scientific, Oxford, UK) equipped with a 9cm diameter gradient coil insert (490mT/m, 175 $\mu$ S; Resonance Research, Billerica, MA). The magnet was interfaced to a Bruker AVANCE console (Bruker, Billerica, MA). Spectra were obtained from a 14mm diameter surface radiofrequency coil tuned to <sup>1</sup>H (400MHz). <sup>13</sup>C-inversion and decoupling radiofrequency pulses (100MHz) were delivered by two orthogonally positioned coils driven in quadrature. Localized <sup>1</sup>H-[<sup>13</sup>C]-NMR spectra were obtained from a volume of 180 $\mu$ L (6x5x6 mm<sup>3</sup>), centered

in the middle of the cortex. Field homogeneity was optimized by adjustment of first and second-order shims using the automated FASTMAP algorithm (16) achieving a line-width-at-half-height of 15Hz. Localization was achieved with the LASER pulse sequence and water suppression by CHESS 4 (17-19). Spectra were collected with repetition a time of 2.5s (20). At the end of the experiment, animals were removed from the magnet and brains were frozen *in situ* using liquid nitrogen while mechanical ventilation was continued to preserve labile metabolites (21; 22).

Brain extracts and plasma samples for high resolution NMR spectroscopy were prepared using a procedure described previously (23; 24). Metabolite concentrations and <sup>13</sup>C-enrichments were measured using <sup>1</sup>H-[<sup>13</sup>C] NMR at 11.7T on a Bruker Avance vertical bore spectrometer.

**Metabolic modeling:** Metabolic fluxes were determined by fitting the two-compartment model of astrocytic and neuronal metabolism depicted in Figure 1, which is based on the time courses of <sup>13</sup>C-enrichment of the C4 position of glutamate and glutamine (Glu4 and Gln4) during the infusion of [2-<sup>13</sup>C]-acetate (Figure 3a) and the <sup>13</sup>C-enrichment of Glu3 and Gln3 at the end of infusion (Figure 3b). For a driver function, the measured time course of [2-<sup>13</sup>C]-acetate in the brain was used instead of the plasma acetate levels to eliminate uncertainties associated with acetate transport kinetics. Mass and isotopic flows from [2-<sup>13</sup>C]-acetate to glial and neuronal Glu and Gln pools were expressed as coupled differential equations (see the supplementary materials available in the online appendix at <http://diabetes.diabetesjournals.org>) within the CWave 3.0 software package

(25) running in Matlab 7.0 (Mathworks, Natick, MA). The equations were solved using a first-/second-order Runge-Kutta algorithm and fitting optimization was achieved using simulated annealing hybridized with a Levenberg-Marquardt algorithm (26) with fixed values for  $V_{\text{cycle}}/V_{\text{tcaN}}$  and  $V_{\text{kbN}}$ . The  $V_{\text{cyc}}/V_{\text{tcaN}}$  ratio was calculated from the steady-state  $^{13}\text{C}$  percentage enrichments of Glu4 and Gln4 from  $[2-^{13}\text{C}]$ -acetate according to the following equation (24):

$$V_{\text{cyc}}/V_{\text{tcaN}} = (\text{Glu4}_N - c_i) / (\text{Gln4}_A - \text{Glu4}_N) \quad (1)$$

where 'N' and 'A' designate the neuronal and astroglial compartments. We assumed that glutamate was distributed between neurons (90%) and astroglia (10%) and glutamine was located entirely in astroglia. The steady-state enrichment of astroglial  $\text{Glu4}_A$  was assumed to equal that of  $\text{Gln4}$ ; thus, the percentage enrichment of neuronal glutamate is given by  $\text{Glu4}_N = (\text{Glu4} - \text{Gln4} * 0.1) / 0.9$ .

The correction factor ' $c_i$ ' removes contributions to  $\text{Glu4}_N$  (at the level of acetyl-CoA) from metabolism of  $^{13}\text{C}$ -labeled plasma products derived from  $[2-^{13}\text{C}]$ -acetate metabolism in peripheral tissues, e.g., plasma glucose-C1 (and/or lactate-C3) and beta-hydroxybutyrate (BHB)-C4/C2 (for details on calculation of this correction factor see Supplemental Materials).

**Statistical analysis:** The error distributions were reported as standard error (S.E.). P-values were calculated using student's t-test using Microsoft Excel, and a  $p \leq 0.05$  was considered to be statistically significant. Monte-Carlo analysis of each animal's data set was performed with CWave to assess the distribution of uncertainties in the model parameters for individual animals (27) (See supplemental online materials). The uncertainties in Monte Carlo fitting were

smaller than the group variabilities for each parameter reported in this study, indicating that treatment differences were not obscured by uncertainties associated with data fitting.

## RESULTS

### Effect of recurrent hypoglycemia on acetate metabolism under euglycemia:

Within 1 minute of initiating the  $[2-^{13}\text{C}]$ -acetate infusion, a steady state plasma level of  $\sim 10\text{mM}$  was reached and maintained throughout the 100 minute experiment. There was rapid  $^{13}\text{C}$ -labeling of plasma BHB at the C4 position (reaching  $\sim 18\%$ ) and at the C3 position of plasma lactate ( $\sim 2.5\%$ ) in both control as well as 3dRH pretreated animals. A 30% increase in blood glucose concentration occurred in both groups during the acetate infusion, without any detectable  $^{13}\text{C}$ -labeling of glucose (Table 1). Brain  $[2-^{13}\text{C}]$ -acetate accumulation in the *in vivo* NMR spectra was immediately observed, suggesting that metabolic flux would not be limited by blood brain barrier transport of acetate in either group (Table 2). While animals from both groups showed similar plasma glucose levels, exposure to antecedent recurrent hypoglycemia resulted in 34% higher brain glucose concentrations (ctrl  $1.27 \pm 0.04 \mu\text{mol/g}$  and 3dRH  $1.72 \pm 0.08 \mu\text{mol/g}$ ;  $p=0.002$ ), suggesting an increased glucose transport capacity in the 3dRH group.

The  $V_{\text{cyc}}/V_{\text{tcaN}}$  ratio, representing the coupling between glutamate/glutamine cycling and the neuronal TCA cycle has no significant change after exposure to recurrent hypoglycemia  $0.58 \pm 0.05$  in comparison to controls  $0.51 \pm 0.03$  ( $p=0.15$ ). Figure 4 (top panel) shows the group averages for  $^{13}\text{C}$  time courses of Glu4 and Gln4 during  $[2-^{13}\text{C}]$ -acetate infusion in control and 3dRH animals

under euglycemia. Individual time courses served as the input for the metabolic model.

While brain acetate metabolism ( $CMR_{ac}$ ) did not differ significantly between 3dRH and control animals (ctrl  $0.15 \pm 0.01 \mu\text{mol/g/min}$  vs. 3dRH  $0.16 \pm 0.01 \mu\text{mol/g/min}$ ;  $p=0.2$ ), brain glucose metabolism ( $CMR_{gl}$ ) under euglycemia was increased in the 3dRH animals by  $43 \pm 4\%$  (ctrl  $0.46 \pm 0.3 \mu\text{mol/g/min}$  vs. 3dRH  $0.66 \pm 0.5 \mu\text{mol/g/min}$ ;  $p=0.003$ ) (Figure 5a). This increase was further reflected by a 50% increase of PDH-flux ( $V_{pdhN}$ ) in the neuronal compartment ( $0.70 \pm 0.08 \mu\text{mol/g/min}$  vs.  $1.06 \pm 0.09 \mu\text{mol/g/min}$ ;  $p=0.008$ ), suggesting an overall increased capacity to utilize glucose. Total brain TCA cycle activity increased as a consequence ( $1.03 \pm 0.05 \mu\text{mol/g/min}$  vs.  $1.45 \pm 0.07 \mu\text{mol/g/min}$ ;  $p < 0.004$ ). Because the metabolism of labeled acetate does not result in  $^{13}\text{C}$  label flow through pyruvate dehydrogenase,  $V_{pdhN}$  is instead calculated by the metabolic model based on several dilutional fluxes, with the main contribution coming from unlabeled glucose.

**Effect of recurrent hypoglycemia on neuronal PDH-flux under euglycemia:** The plasma glucose level during the co-infusion of [ $1-^{13}\text{C}$ ]-glucose and unlabeled acetate was maintained at  $9 \pm 1 \text{mM}$  in the control and  $8.1 \pm 0.8 \text{mM}$  in the 3dRH group;  $p=0.11$ . Throughout, acetate concentrations were comparable between the groups as well as in comparison to the labeled acetate infusions, described above. In contrast, we did not observe labeling of BHB, but a significantly higher degree of [ $3-^{13}\text{C}$ ]-lactate labeling in the plasma (control  $9.5 \pm 0.4\% \text{fE}$  vs. 3dRH  $6.4 \pm 0.06\% \text{fE}$ ;  $p=0.02$ ).

The rate of isotopic enrichment of the brain glutamate pool was considerably higher than that of glutamine (Figure 4), a

reflection of the metabolic compartmentalization and the higher contribution of glucose derived metabolites to neuronal metabolism. Since lactate uses the same metabolic pathway as glucose in the brain, it equally contributes to neuronal PDH-flux ( $V_{pdhN}$ ). The two-compartment model, using the  $^{13}\text{C}$ -time courses of plasma glucose and lactate as well as brain Glu4 and Gln4, was therefore used to calculate  $V_{pdhN}$ . Comparing results from the [ $2-^{13}\text{C}$ ]-acetate infusion with this direct determination of  $V_{pdhN}$  using [ $1-^{13}\text{C}$ ]-glucose revealed essentially the same values: (control  $0.75 \pm 0.05 \mu\text{mol/min/g}$  and 3dRH:  $1.09 \pm 0.07 \mu\text{mol/min/g}$ ;  $p=0.003$ ) (Figure 5a), thereby confirming our finding of increased  $V_{pdhN}$  in the 3dRH group.

**Effect of recurrent hypoglycemia on astrocytic and neuronal metabolism during acute hypoglycemia:** In this experiment the hyperinsulinemic-hypoglycemic clamp maintained plasma glucose levels constant at  $2.1 \pm 0.2 \text{mM}$  in both groups during the infusion of [ $2-^{13}\text{C}$ ]-acetate (Figure 2). In keeping with a loss of counterregulatory responses in the 3dRH model, a 20% higher glucose infusion rate was required in these animals to maintain the same degree of glycemia. The other physiological parameters were controlled at similar levels and plasma concentrations of acetate, lactate and BHB were comparable between groups (Table 1). The most striking change was a decrease in BHB labeling from  $17.9 \pm 3.9\%$  to  $3.3 \pm 1.9\%$  ( $p < 0.001$ ) following exposure to recurrent hypoglycemia (Table 2), consistent with the presence of reduced peripheral ketones in the context of increased peripheral acetate utilization. Furthermore, during hypoglycemia brain concentrations

of GABA in 3dRH rats were increased by 50% ( $p=0.05$ ) as compared to controls, without significant changes of  $^{13}\text{C}$ -enrichment of GABA. When comparing the time courses of Glu4 and Gln4 for the 3dRH and control group, we observed no obvious differences in the rates of Gln4 labeling and only small changes in Glu4 labeling (Figure 4c).

We constrained two parameters in fitting the metabolic model to the time course data: the ratio of glutamate neurotransmitter cycling to neuronal TCA cycle flux,  $V_{\text{cyc}}/V_{\text{TcaN}}$ , and the rate of neuronal ketone body utilization,  $V_{\text{kbN}}$ . In the present study blood BHB enrichment was 17.9% and 3.3% at the end of the [2- $^{13}\text{C}$ ]-acetate infusion in hypoglycemic control and 3dRH animals, respectively; which led to relatively small contributions (and corrections in Eqn. 1; Supplementary Materials) of 2.1% ( $=100 \times 0.179 \times 0.12$ ) and 0.2% ( $=100 \times 0.033 \times 0.12$ ). Including these corrections in Eqn.1 had only minor and insignificant ( $P=0.17$ ) effects on the calculated values of  $V_{\text{cyc}}/V_{\text{TcaN}}$  for the control ( $0.52 \pm 0.07$ ) and RH ( $0.64 \pm 0.09$ ) animals.  $V_{\text{kbN}}$  was set to  $0.04 \pm 0.02$  (3dRH) and  $0.04 \pm 0.01$  (control) based on individual plasma BHB concentrations.

Together with the brain [2- $^{13}\text{C}$ ]-acetate concentration, the time courses of label appearance in  $^{13}\text{C}$  brain acetate, plasma BHB, brain Glu4, Gln4 and endpoints of Glu3, Gln3 we determined the metabolic fluxes of 3dRH vs. control animals under hypoglycemic clamp conditions (Figure 5b): While we observed a  $24 \pm 5\%$  lower  $V_{\text{pdhN}}$  in 3dRH animals compared to controls ( $p=0.004$ ) and a decrease in total TCA cycle flux ( $1.12 \pm 0.02 \mu\text{mol}/\text{min}/\text{g}$  vs.  $0.91 \pm 0.08 \mu\text{mol}/\text{min}/\text{g}$ ;  $p=0.007$ ), the other parameters remained similar between the groups ( $\text{CMR}_{\text{ac}}$ ,  $p=0.2$ ;  $V_{\text{gln}}$ ,  $p=0.3$ ;  $V_{\text{pdhA}}$ ,  $p=0.4$ ; and  $V_{\text{cyc}}$ ,  $p=0.2$ ).

Comparing metabolic fluxes of control animals under euglycemic and hypoglycemic conditions, we found no significant changes in overall brain acetate metabolism ( $\text{CMR}_{\text{ac}}$ ) ( $p=0.5$ ). In controls brain glucose consumption ( $\text{CMR}_{\text{gl}}$ ) in response to hypoglycemia was increased by  $16 \pm 1\%$  ( $p<0.05$ ), mostly due to an increase in glucose related fluxes in the neuronal compartment, namely  $V_{\text{pdhN}}$  ( $37 \pm 3\%$ ) ( $p<0.01$ ) and  $V_{\text{TcaN}}$  ( $40 \pm 3\%$ ) ( $p=0.05$ ). In contrast astroglial glucose uptake  $V_{\text{pdhA}}$  was decreased by  $32 \pm 5\%$  ( $p=0.01$ ), suggesting a redistribution of glucose consumption to maintain neuronal function, as reflected by a preserved brain total TCA cycle activity (Figure 5b).

Similar to controls, 3dRH animals showed no changes in  $\text{CMR}_{\text{ac}}$ . However in a response opposite to controls a significant  $40 \pm 5\%$  decrease in  $\text{CMR}_{\text{gl}}$  ( $p<0.001$ ) was observed in response to hypoglycemia (Figure 5b). Glucose flux in the astrocytic compartment dropped by  $75 \pm 20\%$  ( $V_{\text{pdhA}}$ ) ( $p<0.001$ ), in neurons by  $36 \pm 4\%$  ( $V_{\text{pdhN}}$ ) ( $p=0.005$ ). The combined effect of these decreases in both compartments is a resultant total brain TCA cycle activity decrease by  $37 \pm 4\%$  ( $p=0.001$ ). Comparing the relative contributions of acetate and glucose when going from eu- to hypoglycemia ( $\text{CMR}_{\text{ac}}/\text{CMR}_{\text{gl}}$ ), the control group showed a 12% decrease ( $p=0.06$ ), while 3dRH rats revealed 24% increase ( $p=0.006$ ), indicating an increased relative contribution of acetate to brain metabolism in 3dRH animals under hypoglycemic conditions. In this context, however, it is important to note that at baseline euglycemic conditions 3dRH animals already show a 43% higher degree of brain glucose consumption ( $\text{CMR}_{\text{gl}}$ ) than control animals ( $p=0.004$ ).



## DISCUSSION

In this study we measured the rates at which glucose and an alternate fuel (acetate) is oxidized under different glycemic conditions. Measurements of brain metabolism in animals exposed to recurrent hypoglycemia resulted in two main observations. First, after antecedent recurrent hypoglycemia basal brain glucose metabolism at euglycemia is *increased* in comparison to controls. This increase was mainly attributable to higher *neuronal* glucose oxidation, suggesting that, when glucose is present in sufficient amounts, neurons are better able to use glucose. Second, under standardized relatively severe hypoglycemic conditions 3dRH animals showed a decrease in brain glucose consumption in neurons and astroglia, which contrasts with control animals in which neuronal glucose metabolism was preserved (Fig. 5a). Thus, there is a fundamentally different metabolic response of neurons to hypoglycemia between 3dRH and control animals: While acetate consumption remained comparable under eu- and hypoglycemia in both groups, acetate comprised a greater relative contribution to total brain oxidation.

Controversy exists regarding the relative degree of cognitive impairment caused by acute hypoglycemia in patients with type 1 diabetes as compared to non-diabetic subjects (for a recent review see (28)). This may be in part a consequence of metabolic adaptations that occur in response to different degrees of antecedent exposure to hypoglycemia (29; 30). In a previous study using the same rodent model, 3dRH animals subjected to a spatial memory test under euglycemia performed better than controls, while they did worse during acute hypoglycemia (9). The current observation of higher total

TCA cycle activity under euglycemia and lower activity under hypoglycemia in 3dRH animals parallels this biological effect. The better performance under euglycemia in 3dRH animals may be related, in part, to changes in glucose transport across the blood brain barrier, resulting in a higher brain glucose level at comparable plasma glucose, an effect we also observed using microdialysis in previous studies of our 3dRH model (9; 15). The 34% increase in brain glucose levels measured here in the 3dRH group at euglycemia is consistent with the 17% increase reported in type 1 diabetic patients with hypoglycemia unawareness at euglycemia (10). Furthermore, our data establish that the higher brain glucose concentration is not the consequence of a decrease in glucose utilization, but instead occurs despite accelerated brain glucose metabolism.

To overcome the relative uncertainty associated with using [2-<sup>13</sup>C]-acetate, a predominantly glial fuel, for the calculation of glucose consumption, we performed a confirmatory experiment with [1-<sup>13</sup>C]-glucose as a substrate. The measured neuronal PDH-flux in 3dRH animals ( $1.06 \pm 0.10 \mu\text{mol}/\text{min}/\text{g}$  ([2-<sup>13</sup>C]-acetate) vs.  $1.09 \pm 0.07 \mu\text{mol}/\text{min}/\text{g}$  ([1-<sup>13</sup>C]-glucose)) was the same for both substrates, further supporting the accuracy of our metabolic model.

In this animal study, transporter kinetics were saturated by an infusion of [2-<sup>13</sup>C]-acetate at a level higher than is ethically and technically permissible in comparable human studies. The acetate infusion resulted in reliable brain acetate measurements, which then allowed us to accurately determine metabolic fluxes independent of potential changes in monocarboxylic acid transport transporter activity at the blood brain barrier, which

are anticipated in the context of exposure to recurrent hypoglycemia (13).

In the present study all animal groups (euglycemic and hypoglycemic) showed  $^{13}\text{C}$  labeling of BHB from  $[2\text{-}^{13}\text{C}]$ -acetate (Table 1), likely due to its rapid metabolism in the liver. BHB labeled with  $^{13}\text{C}$  at C4 and C2 would contribute to  $^{13}\text{C}$  labeling of glutamate-C4, as well as other carbon positions. At euglycemia (control and 3dRH) plasma BHB levels were low ( $\sim 0.3$  mM), such that labeling of glutamate-C4 would be negligible. However, during hypoglycemia baseline BHB levels were elevated ( $\sim 1$  mM), as animals were fasted overnight to reduce their liver glycogen content. The lower rate of brain glucose utilization in hypoglycemic 3dRH animals is not likely due to increased consumption of ketone bodies. BHB levels were the same in both groups and brain levels were not detected, implying similar blood-to-brain concentration gradients - the driving force for BHB utilization in the brain. Furthermore, if BHB utilization had been greater in 3dRH compared to control animals, there would have been greater dilution of brain glutamate-C4 enrichment relative to control animals, which was not seen (14.3% vs. 13.9%,  $P=0.14$ ; Table 2).

The contribution of acetate to astroglial TCA cycle flux ( $\text{CMR}_{\text{ac}}/V_{\text{tcaA}}$ ) under hypoglycemia was increased by 50% in both control and 3dRH animals as compared to euglycemia. A similar value for the ratio  $\text{CMR}_{\text{ac}}/V_{\text{tcaA}}$  was reached in both groups (CTRL:  $0.71 \pm 0.19$ ; 3dRH  $0.67 \pm 0.26$ ), suggesting that acetate metabolism was saturated in each case. This value is very similar to the maximal value predicted for  $\text{CMR}_{\text{ac}}/V_{\text{tcaA}}$  in human subjects with type 1 diabetes ( $0.69 \pm 0.17$ ) (13). Assuming that our rat model of recurrent hypoglycemia mimics relevant features of glial metabolism in humans,

the difference noted previously between type 1 diabetic and control subjects are likely related to an increase in transporter activity.

It is possible that reduced neuronal TCA cycle activity in the context of preserved glycolytic flux may have caused the elevated lactate levels we observed in the brains of 3dRH animals under hypoglycemia. This lactate was less enriched and could have been either derived from endogenous brain glycogen stores or directly from unlabeled brain glucose. However, since our model does account for labeled as well as unlabeled lactate as a contribution to neuronal PDH flux and the final labeled glutamate and glutamine pools were comparable; these possibilities are not likely explanations for the significant decrease in  $V_{\text{pdhN}}$  we observed.

3dRH animals showed higher GABA levels during acute hypoglycemia, which was not observed in control animals (Table 2). Other studies from our group have, in fact, demonstrated a 3-fold increase in GABA in hypothalamic interstitial fluid (31) and increased long term potentiation in hippocampal slice preparations in rats exposed to recurrent hypoglycemia (32). Since GABA is an inhibitory neurotransmitter and increased levels could reduce neuronal activity as well as metabolic demand under hypoglycemic conditions in 3dRH animals, this could be a cause of the reduced neuronal TCA cycle activity we observed in our study.

In summary, our study provides the first evidence that recurrent hypoglycemia increases neuronal glucose metabolism under euglycemia. Under hypoglycemia glucose metabolism decreases while acetate utilization remains constant, the latter supporting a greater relative fraction of total oxidative metabolism. Neuron

specific alternate fuels may therefore provide a means of reducing the risk of hypoglycemia-induced brain injury in intensively-treated diabetic patients.

**ACKNOWLEDGEMENTS:**

The authors wish to thank Terry Nixon and Scott McIntyre of the MRRC Engineering Core for maintenance of the NMR spectrometer and technical support, Peter Brown for design and fabrication of the NMR probe and transceiver coils, Bei Wang for animal surgery and Wanling Zhu for recurrent hypoglycemia treatment. This work was supported in part by grants from the National Institutes of Health, NIDDK R01 DK027121 (K.L.B.), NINDS R01 NS037527, NS051854-01 (D.L.R.), NIDDK R37 DK20495, and the Juvenile Diabetes Research Foundation 4-2004-807 (R.S.S.). R.H was supported by a Ruth Kirschstein NRSA from the NIDDK, F32 DK077461 and G.F.M. by K02 AA-13430. We also gratefully acknowledge NIH grants, NINDS 1 P30 NS052519 and the QNMR Program for NMR spectrometer and facilities support and NIDDK P30 DK45735 of the Yale Diabetes Endocrinology Research Center (DERC).

**Legends:**

Figure 1. Two compartment model of the contribution of infused labeled acetate ( $[2-^{13}\text{C}]\text{-Ac}$ ) to astroglial and neuronal metabolism. Modified after Lebon et al.(33).

Figure 2. Hypoglycemic-hyperinsulinemic clamp.

(a) Plasma glucose concentration. (b) Glucose infusion rate. (black diamonds = controls, white diamonds = 3dRH); The time point at  $t=0$  min indicates the beginning of the  $^{13}\text{C}$ -labeled acetate infusion and spectral acquisition; error bars represent standard error (S.E.).

Figure 3 NMR spectra.

a) Representative stack of *in vivo*  $^1\text{H}$ - $[^{13}\text{C}]$  difference spectra acquired over time revealing gradual accumulation of brain  $[2-^{13}\text{C}]\text{-acetate}$  and its subsequent appearance in the stable metabolite pools of Glu4, Glu3 and Gln4, Gln3

b) Representative high resolution  $^1\text{H}$ - $[^{13}\text{C}]$  spectra of brain tissue extracts used to further resolve the metabolite concentrations and enrichments of different carbon position of Glutamate-C4,3,2 (Glu<sub>4,3,2</sub>); Glutamine-C4,3,2 (Gln<sub>4,3,2</sub>); GABA-C2,3,4, Aspartate-C3 (Asp<sub>3</sub>); Alanine-C3 (Ala<sub>3</sub>) and Lactate-C3 (Lac<sub>3</sub>). Combination of these two measurements revealed the time courses of label accumulation in these metabolite pools, which were then used in the two compartment model of brain metabolism to determine the metabolic fluxes.

Figure 4. Time courses of Glu4 and Gln4 labeling during labeled substrate infusions.

a)  $[2-^{13}\text{C}]\text{-acetate}$  at euglycemia. b)  $[1-^{13}\text{C}]\text{-glucose}$  and unlabeled acetate at euglycemia. c)  $[2-^{13}\text{C}]\text{-acetate}$  at hypoglycemia. Group averaged data is depicted in the upper panels while representative individual animals with best fits of the two-compartment metabolic model appear in lower panels.

(Black diamonds = Gln4 control; white diamonds = Gln4 3dRH; black squares = Glu4 control; white squares = Glu4 3dRH). Error bars represent standard error (S.E.).

Figure 5. Metabolic fluxes derived from two-compartment model.

a) in control and 3DRH animals under eu- and hypoglycemia. Black bars = control group at euglycemia; gray bars = control group at hypoglycemia; white bars = 3dRH at euglycemia; hatched bars = 3dRH at hypoglycemia.

b) Percentage change in metabolic rates from eu- to hypoglycemia within groups,  $((\text{euglycemia} - \text{hypoglycemia})/\text{euglycemia}) \times 100$ . (Black bars = control group; white bars = 3dRH group).

**REFERENCES:**

1. DCCT: The effect of intensive treatment of diabetes on the development and progression of long-term complications in insulin-dependent diabetes mellitus. The Diabetes Control and Complications Trial Research Group. *N Engl J Med* 329:977-986, 1993
2. UKPDS: Intensive blood-glucose control with sulphonylureas or insulin compared with conventional treatment and risk of complications in patients with type 2 diabetes (UKPDS 33). UK Prospective Diabetes Study (UKPDS) Group. *Lancet* 352:837-853, 1998
3. Amiel SA, Sherwin RS, Simonson DC, Tamborlane WV: Effect of intensive insulin therapy on glycemic thresholds for counterregulatory hormone release. *Diabetes* 37:901-907, 1988
4. Cryer PE: Iatrogenic hypoglycemia as a cause of hypoglycemia-associated autonomic failure in IDDM. A vicious cycle. *Diabetes* 41:255-260, 1992
5. Cryer PE: Hypoglycemia risk reduction in type 1 diabetes. *Exp Clin Endocrinol Diabetes* 109 Suppl 2:S412-423, 2001
6. Cryer PE: Banting Lecture. Hypoglycemia: the limiting factor in the management of IDDM. *Diabetes* 43:1378-1389, 1994
7. Ferguson SC, Blane A, Wardlaw J, Frier BM, Perros P, McCrimmon RJ, Deary IJ: Influence of an early-onset age of type 1 diabetes on cerebral structure and cognitive function. *Diabetes Care* 28:1431-1437, 2005
8. Warren RE, Frier BM: Hypoglycaemia and cognitive function. *Diabetes Obes Metab* 7:493-503, 2005
9. McNay EC, Sherwin RS: Effect of recurrent hypoglycemia on spatial cognition and cognitive metabolism in normal and diabetic rats. *Diabetes* 53:418-425, 2004
10. Criego AB, Tkac I, Kumar A, Thomas W, Gruetter R, Seaquist ER: Brain glucose concentrations in patients with type 1 diabetes and hypoglycemia unawareness. *J Neurosci Res* 79:42-47, 2005
11. Jacob RJ, Dziura J, Blumberg M, Morgen JP, Sherwin RS: Effects of recurrent hypoglycemia on brainstem function in diabetic BB rats: protective adaptation during acute hypoglycemia. *Diabetes* 48:141-145, 1999
12. Powell AM, Sherwin RS, Shulman GI: Impaired hormonal responses to hypoglycemia in spontaneously diabetic and recurrently hypoglycemic rats. Reversibility and stimulus specificity of the deficits. *J Clin Invest* 92:2667-2674, 1993
13. Mason GF, Petersen KF, Lebon V, Rothman DL, Shulman GI: Increased brain monocarboxylic Acid transport and utilization in type 1 diabetes. *Diabetes* 55:929-934, 2006
14. Patel AB, De Graaf RA, Mason GF, Rothman DL, Shulman RG, Behar KL: Coupling of glutamatergic neurotransmission and neuronal glucose oxidation over the entire range of cerebral cortex activity. *Ann N Y Acad Sci* 1003:452-453, 2003
15. Herzog RI, Chan O, Yu S, Dziura J, McNay EC, Sherwin RS: Effect of acute and recurrent hypoglycemia on changes in brain glycogen concentration. *Endocrinology*, 2008
16. Gruetter R, Weisdorf SA, Rajanayagan V, Terpstra M, Merkle H, Truwit CL, Garwood M, Nyberg SL, Ugurbil K: Resolution improvements in in vivo 1H NMR spectra with increased magnetic field strength. *J Magn Reson* 135:260-264, 1998

17. Garwood M, DelaBarre L: The return of the frequency sweep: designing adiabatic pulses for contemporary NMR. *J Magn Reson* 153:155-177, 2001
18. Haase A, Frahm J, Hanicke W, Matthaei D: 1H NMR chemical shift selective (CHESS) imaging. *Phys Med Biol* 30:341-344, 1985
19. Scheenen TW, Klomp DW, Wijnen JP, Heerschap A: Short echo time 1H-MRSI of the human brain at 3T with minimal chemical shift displacement errors using adiabatic refocusing pulses. *Magn Reson Med* 59:1-6, 2008
20. de Graaf RA, Mason GF, Patel AB, Behar KL, Rothman DL: In vivo 1H-[13C]-NMR spectroscopy of cerebral metabolism. *NMR Biomed* 16:339-357, 2003
21. Katsura K, Folbergrova J, Siesjo BK: Changes in labile energy metabolites, redox state and intracellular pH in postischemic brain of normo- and hyperglycemic rats. *Brain Res* 726:57-63, 1996
22. Ponten U, Ratcheson RA, Salford LG, Siesjo BK: Optimal freezing conditions for cerebral metabolites in rats. *J Neurochem* 21:1127-1138, 1973
23. Patel AB, Rothman DL, Cline GW, Behar KL: Glutamine is the major precursor for GABA synthesis in rat neocortex in vivo following acute GABA-transaminase inhibition. *Brain Res* 919:207-220, 2001
24. Patel AB, de Graaf RA, Mason GF, Rothman DL, Shulman RG, Behar KL: The contribution of GABA to glutamate/glutamine cycling and energy metabolism in the rat cortex in vivo. *Proc Natl Acad Sci U S A*, 2005
25. Mason GF, Falk Petersen K, de Graaf RA, Kanamatsu T, Otsuki T, Shulman GI, Rothman DL: A comparison of (13)C NMR measurements of the rates of glutamine synthesis and the tricarboxylic acid cycle during oral and intravenous administration of [1-(13)C]glucose. *Brain Res Brain Res Protoc* 10:181-190, 2003
26. Alcolea A, Carrera J, Medina A: A hybrid Marquardt-Simulated Annealing method for solving the groundwater inverse problem. *Proceedings of the ModelCARE 99 IAHS Publ Number* 265:157-163, 2000
27. Mason GF, Behar KL, Rothman DL, Shulman RG: NMR determination of intracerebral glucose concentration and transport kinetics in rat brain. *J Cereb Blood Flow Metab* 12:448-455, 1992
28. Kodl CT, Seaquist ER: Cognitive dysfunction and diabetes mellitus. *Endocr Rev* 29:494-511, 2008
29. Sommerfield AJ, Deary IJ, McAulay V, Frier BM: Short-term, delayed, and working memory are impaired during hypoglycemia in individuals with type 1 diabetes. *Diabetes Care* 26:390-396, 2003
30. Widom B, Simonson DC: Glycemic control and neuropsychologic function during hypoglycemia in patients with insulin-dependent diabetes mellitus. *Ann Intern Med* 112:904-912, 1990
31. Chan O, Cheng H, Herzog R, Czyzyk D, Zhu W, Wang A, McCrimmon RJ, Seashore MR, Sherwin RS: Increased GABAergic tone in the ventromedial hypothalamus contributes to suppression of counterregulatory responses after antecedent hypoglycemia. *Diabetes* 57:1363-1370, 2008
32. McNay EC, Williamson A, McCrimmon RJ, Sherwin RS: Cognitive and neural hippocampal effects of long-term moderate recurrent hypoglycemia. *Diabetes* 55:1088-1095, 2006

33. Lebon V, Petersen KF, Cline GW, Shen J, Mason GF, Dufour S, Behar KL, Shulman GI, Rothman DL: Astroglial contribution to brain energy metabolism in humans revealed by <sup>13</sup>C nuclear magnetic resonance spectroscopy: elucidation of the dominant pathway for neurotransmitter glutamate repletion and measurement of astrocytic oxidative metabolism. *J Neurosci* 22:1523-1531, 2002

		Euglycemia				Hypoglycemia			
		Control		3dRH		Control		3dRH	
		<i>before</i>	<i>after</i>	<i>before</i>	<i>after</i>	<i>before</i>	<i>after</i>	<i>before</i>	<i>after</i>
pH		7.37±0.02	7.40±0.03	7.36±0.01	7.35±0.02	7.38±0.01	7.43±0.01	7.40±0.01	7.47±0.02* <sup>§</sup>
pCO <sub>2</sub>	(mmHg)	38±1	45±2	41±4	44±4	35±3	38±2	35±3	37±4
pO <sub>2</sub>	(mmHg)	130±7	120±5	148±5	147±9	130±10	170±15	130±10	160±15
glucose	mM	9.4±0.7	12.5±1.1	8.1±0.03	11±0.3	2.3±0.2	2.0±0.2	2.3±0.7	2.3 ±0.7
	%E	0	n.d.	0	n.d.	0	n.d.	0	n.d.
BHB	mM	0.3±0.03	0.5±0.1	0.3±0.03	0.37±0.07	1.2±0.07	0.9±0.06	1.2±0.6	0.7±0.4
	%E	0	18±0.7	0	17±5	0	17.9± 1.3	0	3.3±1.9
Lactate	mM	1.3±0.1	1.6±0.3	1.0±0.07	1.20±0.02	1.0±0.07	0.8±0.07	1.0±0.2	0.8±0.4
	%E	0	2.6±0.4	0	2.5±0.7	0	n.d.	0	n.d.
Acetate	mM	0.13±0.01	9.6±0.9	0.14±0.02	10.6±1.5	0.13±0.02	8.2±2	0.14	11±5
	%E	0	90±0.7	0	88±1.3	0	86±2	0	84±6

**Table 1.** Effect of [2-<sup>13</sup>C]-acetate infusions on physiological variables and substrates (concentrations and <sup>13</sup>C-enrichments) measured in arterial plasma of control and 3dRH rats under euglycemic and hypoglycemic conditions. The natural abundance of <sup>13</sup>C (1.1%) was subtracted from the percentage enrichments (%E). (\*P-values for control Vs 3dRH ( <sup>\*</sup>p<0.05, <sup>\*\*</sup>p<0.01), <sup>§</sup>P values for Euglycemia vs. Hypoglycemia, <sup>§</sup>p<0.05, <sup>§§</sup>p<0.01); n.d. = non-detectable



**Table 2.** Brain extract metabolite concentrations ( $\mu\text{mol/g}$ ) and  $^{13}\text{C}$ -percentage enrichments (%E) at the end of the [2- $^{13}\text{C}$ ]-acetate infusion. The natural abundance of  $^{13}\text{C}$  (1.1%) was subtracted from the percentage enrichments. (\* $P < 0.05$  3dRH vs. control;  $^{\S}P < 0.05$ ,  $^{\S\S}P < 0.01$ , hypoglycemia vs. euglycemia within a group) n.d. = non-detectable.

		Euglycemia		Hypoglycemia	
		Control	3dRH	Control	3dRH
Acetate	conc. [ $\mu\text{mol/g}$ ]	$1.5 \pm 0.2$	$1.2 \pm 0.3$	$1.2 \pm 0.1$	$0.8 \pm 0.2$
	C2 %E	$90 \pm 0.7$	$88 \pm 1.4$	$86 \pm 2$	$84 \pm 2$
Glucose	conc. [ $\mu\text{mol/g}$ ]	$1.27 \pm 0.04$	$1.72 \pm 0.08^*$	$0.35 \pm 0.04$	$0.4 \pm 0.04$
	C1 %E	n.d.	n.d.	n.d.	n.d.
Lactate	conc. [ $\mu\text{mol/g}$ ]	$2.2 \pm 0.2$	$2.3 \pm 0.2$	$1.9 \pm 0.5$	$3.4 \pm 0.3^{*\S}$
	C3 %E	$2.3 \pm 0.2$	$2.6 \pm 0.2$	$3.4 \pm 0.5$	$1.2 \pm 0.4^{*\S}$
Aspartate	conc. [ $\mu\text{mol/g}$ ]	$2.9 \pm 0.1$	$2.7 \pm 0.1$	$3.3 \pm 0.5$	$3.9 \pm 0.5^{*\S}$
	C3 %E	$7.1 \pm 0.8$	$6.5 \pm 0.6$	$5.9 \pm 0.4$	$6.5 \pm 0.8$
Glutamate	conc. [ $\mu\text{mol/g}$ ]	$10.8 \pm 0.5$	$11.5 \pm 0.6$	$11.5 \pm 0.6$	$12.1 \pm 0.8$
	C2 %E	$2.8 \pm 0.3$	$3.2 \pm 0.3$		
	C3 %E	$7.7 \pm 0.4$	$7.6 \pm 0.5$	$8.7 \pm 0.6$	$7.7 \pm 0.7$
	C4 %E	$10.5 \pm 0.3$	$10.8 \pm 0.5$	$13.9 \pm 0.6^{\S}$	$14.3 \pm 1^{\S\S}$
Glutamine	conc. [ $\mu\text{mol/g}$ ]	$6.9 \pm 0.3$	$6.6 \pm 0.3$	$7.2 \pm 0.4$	$7.2 \pm 0.6$
	C2 %E	$7.3 \pm 0.4$	$6.7 \pm 0.3$		
	C3 %E	$11.2 \pm 0.7$	$10.4 \pm 0.2$	$11.5 \pm 0.4$	$10.0 \pm 0.6$
	C4 %E	$23.7 \pm 1.0$	$22.9 \pm 0.8$	$27.8 \pm 0.5^{\S}$	$29 \pm 0.8^{\S}$
GABA	conc. [ $\mu\text{mol/g}$ ]	$1.6 \pm 0.1$	$1.7 \pm 0.2$	$1.8 \pm 0.2$	$2.7 \pm 0.4^{\S\S}$
	C2 %E	$9.2 \pm 0.4$	$10.3 \pm 0.5$	$12.0 \pm 0.3^{\S\S}$	$11.3 \pm 1$
	C3 %E	$5.3 \pm 0.7$	$5.9 \pm 0.4$	$7.3 \pm 0.6$	$5.3 \pm 1.4$
	C4 %E	$6.9 \pm 0.7$	$6.1 \pm 0.3$	$9.2 \pm 1.1^{\S}$	$7.3 \pm 1.2$

Figure 1

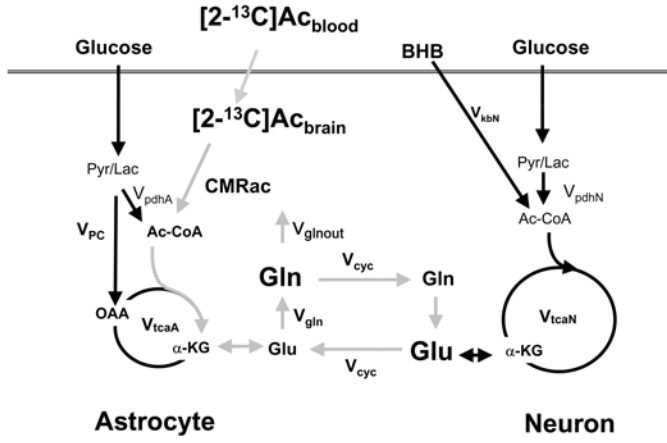


Figure 2

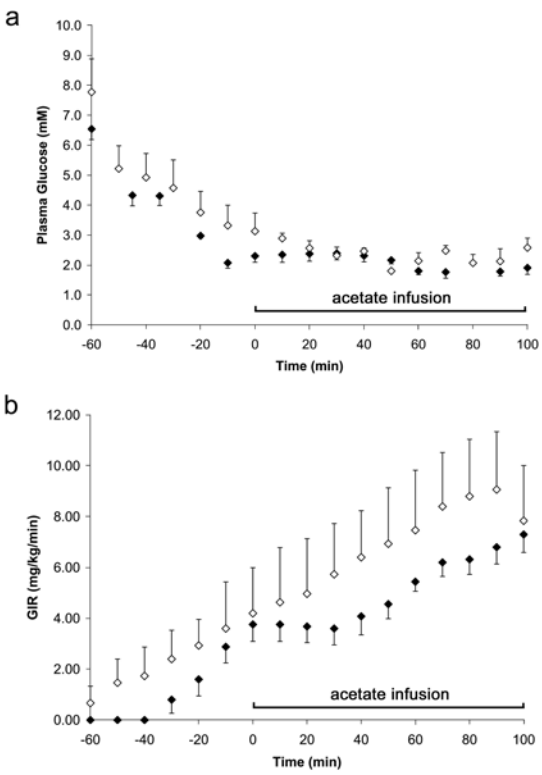


Figure 3:

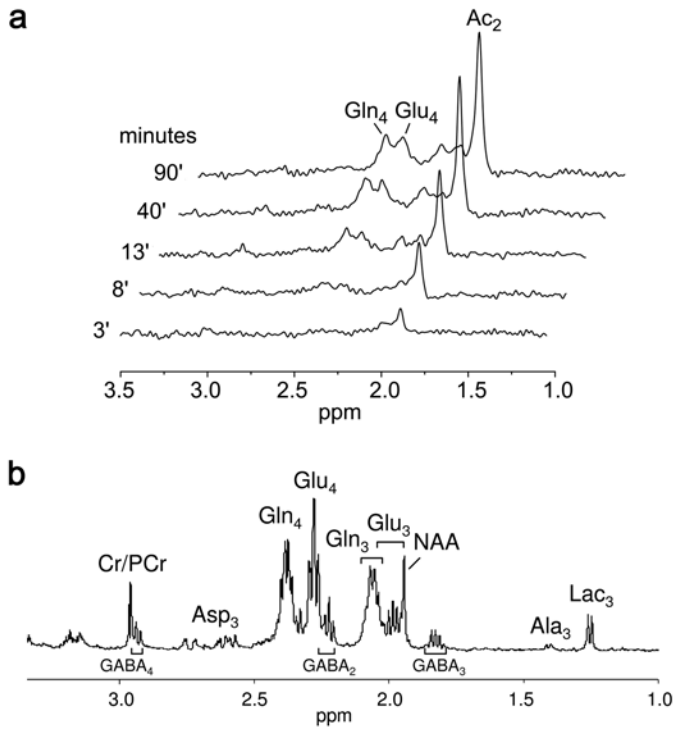


Figure 4

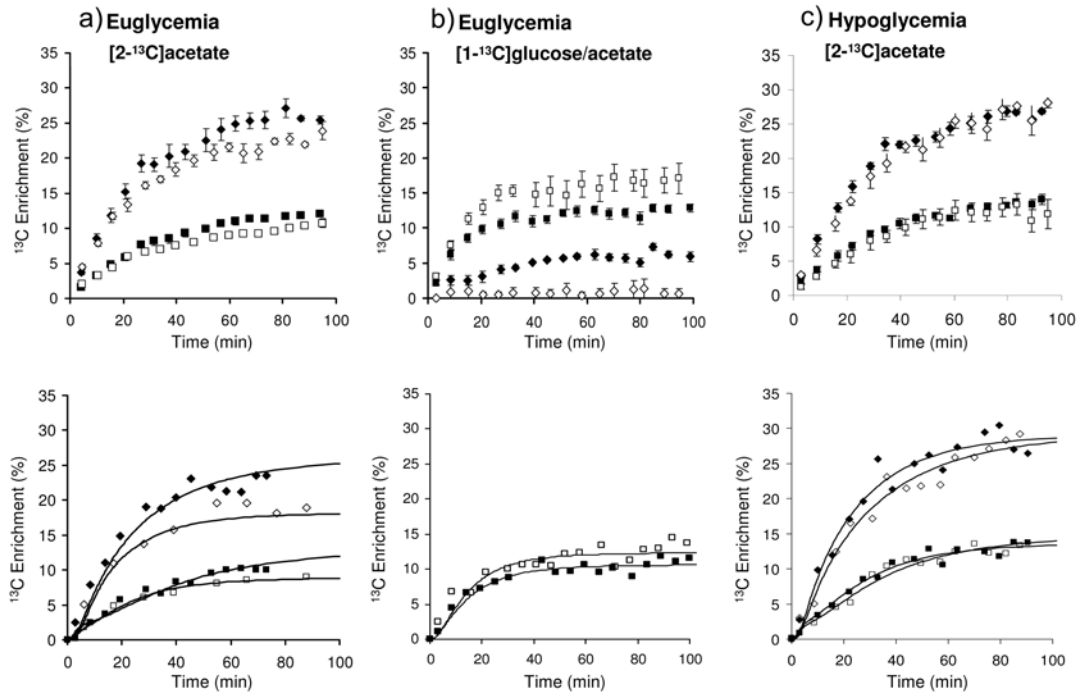


Figure 5

